Hepatic transcriptomics and metabolomics indicated pathways associated with immune stress of broilers induced by lipopolysaccharide

Shicheng Bi ®,*,[1] Jianjian Shao,* Yiwen Qu,* Weidong Hu ®,* Yue Ma,* and Liting Cao ®[#]

Department of Traditional Chinese Veterinary Medicine, College of Veterinary Medicine, Southwest University, Rongchang, Chongqing, 402460, PR China; and [#]Immunology Research Center, Medical Research Institute, Southwest University, Rongchang, Chongqing 402460, PR China

ABSTRACT Broilers with immune stress show decline of growth performance, causing severe economic losses. However, the molecular mechanisms underlying the immune stress still need to be elucidated. One hundred and twenty broiler chicks were randomly assigned to 2 groups with 6 repeats per group, 10 birds per repeat. The model broilers were intraperitoneally injection of 250 μg/kg LPS at 12, 14, 33, and 35 d of age to induce immunological stress. Control group was injected with an equivalent amount of sterile saline. Blood samples from chickens were collected using wing vein puncture at 35 d of age and the serum was obtained for detection of CORT and ACTH. At the end of the experiment, the liver tissues were excised and collected for omics analysis. The results showed that LPS challenge significantly inhibited growth performance, increased relative weight of liver, spleen and decreased relative weight of bursa, as well as enhanced the concentration of serum ACTH and CORT, when compared with the Control. A total of 129 DEGs and a total of 109 differential metabolites were identified between Model and Control group. Transcriptomics profiles revealed that immune stress enhanced the expression of genes related to defense function while declined the expression of genes related to oxidation-reduction process. Metabolomics further suggested that immune stress changed metabolites related to amino acid metabolism, glycerophospholipid metabolism. In addition, integrated analysis suggested that the imbalance of valine, leucine and isoleucine metabolism, glycerophospholipid metabolism, and mTOR signaling pathway played an important role in immune stress of broiler chicks.

Key words: broiler chicks, liver, transcriptome, metabolome, immune stress

INTRODUCTION

Young broilers have an immature immune system and are more susceptible to environmental stressors (Li et al., 2019). High stocking density, contaminated feed, inappropriate management, temperature extremes, and pathogen challenges have a cumulative impact on poultry behavior and physiology, thus leading to the loss of immune homeostasis and triggering immune stress (Liu et al., 2015; Li et al., 2018; Bi et al., 2019). Broilers with immune stress show decline of growth performance, causing severe economic losses (Zheng et al., 2021).

Injection of LPS is a classical approach to establish the model of immune stress in broiler chicks (Liu et al., 2015; Zhang et al., 2017a,b; Li et al., 2018; Yang et al., 2019; Zheng et al., 2021). In response to LPS, the inflammatory cytokines and stress-related hormones will increase while the antioxidant function and growth hormone will decline (Zhang et al., 2017a,b; Yang et al., 2019; Zheng et al., 2021). Cytokines such as interleukin-6 (**IL-6**) may accelerate glycogen hydrolysis and glucose production while tumor necrosis factor alpha (**TNF-α**) may promote adipolysis and proteolysis, leading to reduced deposition of protein and lipid (Hennigar et al., 2017; Patel and Patel, 2017). In addition, inflammatory cytokines induced by LPS could promote glucocorticoid secretion and reduce the secretion of growth hormone through the neuro-endocrine system, resulting in decreased appetite and feed intake (Zhang et al., 2017a, b). Moreover, overproduction of proinflammatory cytokines can generate reactive oxygen species (**ROS**), causing oxidative damage of multiple tissues (Xing et al., 2021). A previous study also demonstrated that lipopolysaccharide (**LPS**) induced immune stress by increasing the phosphorylation of Jun N-terminal kinase (**JNK**), p38 mitogen-activated protein kinase (**MAPK**), nuclear factors kappa B (**NF-κB**) while

decreasing the phosphorylation level of mammalian target of rapamycin (**mTOR**) (Liu et al., 2018). However, the molecular mechanisms underlying the immune stress still need to be elucidated.

Liver is a center of substance and energy metabolism and undertakes principal metabolic processes including synthesis, decomposition, excretion and transformation (Feng et al., 2013). Nevertheless, the liver plays a critical role in nutrient metabolism and nutrient repartitioning after immune challenge (Zheng et al., 2021). Multiomics analysis technologies are increasingly being used to identify potential biomarkers and clarify pathogenesis and mechanisms in relation to diseases (Zhao et al., 2020). Unlike each type of omics data, which typically provides a signal list of differences in disease pathogenesis, multiomics analysis can elucidate potential causative changes that can be further tested by detailed molecular studies, rather than simply reflecting reactive processes (Hasin et al., 2017). In the present study, immune stress of broiler chicks was induced as previously described (Liu et al., 2015). Then, comprehensive analysis of transcriptomics and metabolomics was performed to identify the differentially expressed genes and differential metabolites in liver. The results can help clarify potential metabolic alterations and molecular mechanisms in the immune stressed broilers and provide further information to maintain immune responses and improve disease resistance in poultry.

MATERIALS AND METHODS

Broilers

The animal experiments were performed in accordance with the Animal Care and Use Committee of Southwest University (permit number IACUC-20200701-01). One-day-old male Shaver brown broilers (trade name: hongyu broiler chickens) were purchased from Sichuan Lihua Poultry Co., Ltd. and separately housed into three-layer cages. The cage size was $140 \times 150 \times 60$ cm. The indoor temperature was maintained at 32°C to 34°C for a week, then gradually reduced to 26°C at the rate of 1°C every 2 d through to slaughter. All broilers were provided with feed and water ad libitum.

Reagents

LPS from *E. coli* serotype O55:B5 was purchased from Sigma-Aldrich Chemical Co. (St. Louis, MO). Detection kits for chicken adrenocorticotropic hormone (**ACTH**) (H097-1-1) and corticosterone (**CORT**) (H205-1-2) were purchased from Nanjing Jiancheng Bioengineering Institute (Nanjing, China). All other chemicals were analytic grades.

Experimental Design

One hundred and twenty broiler chicks were randomly assigned to 2 groups with 6 repeats per group, 10 birds per repeat. Broilers were assigned to the basal diet (Table 1). The model broilers were intraperitoneally injected with 250 μg/kg LPS at 12, 14, 33, and 35 d of age to induce immunological stress (Figure 1). Control group was injected with an equivalent amount of sterile saline. Blood samples from chickens were collected using wing vein puncture at 35 d of age and the serum was obtained for detection of CORT and ACTH. At the end of the experiment, the liver tissues were excised and collected for omics analysis.

Growth Performance

Birds were group weighed by cage every week and feed intake on a cage basis was recorded daily to calculate average daily weight gain (**DWG**), daily feed intake (**DFI**) and feed conversion ratio (**FCR**) for each period.

Relative Weights of Organs

At 42 d of age, 5 birds from each replicate were randomly weighed and killed by cervical dislocation. The liver, spleen, and bursa were removed and the organ weights were immediately measured. The results were expressed relative to body weight (**BW**) (g of organ/kg of BW).

Determination of CORT and ACTH

At 35 d of age, 5 birds in each replicate of per treatment were randomly selected for blood collection. Then, 1 mL of blood was centrifuged at 3,000 g for 10 min to get serum. The concentration of serum CORT and

Table 1. Dietary formulation of basal diet.[1]

Item	%
Composition	
Corn	55.35
Soybean meal	29.00
Wheat shorts	2.70
Fish meal	5.01
Rapeseed oil	3.17
Salt	0.27
Dicalcium phosphate	3.13
Limestone	0.15
DL-Met	0.12
Lys	0.10
Premix[2]	1
Total	100
Nutrient	
Crude Protein	21.10
Crude fibre	2.24
Ca	0.92
Total phosphorus	1.20
Methionine	0.12
Sodium chloride	0.27

[1]Value were calculated from data provided by Feed Database in China (2013).

[2]Each kilogram of premix compound contained: vitamin A, 7,000 IU; vitamin D_3, 2,500 IU; vitamin E, 30 mg; vitamin K_3, 1 mg; vitamin B_1, 1.5 mg; vitamin B_2, 4 mg; vitamin B_6, 2 mg; vitamin B_{12}, 0.02 mg; niacin, 30 mg; folic acid, 0.55 mg; pantothenic acid, 10 mg; biotin, 0.16 mg; choline chloride, 400 mg; Cu, 20 mg; Fe, 70 mg; Mn, 100 mg; Zn, 70 mg; I, 0.4 mg, Se, 0.5 mg, and virginiamycin, 20 mg.
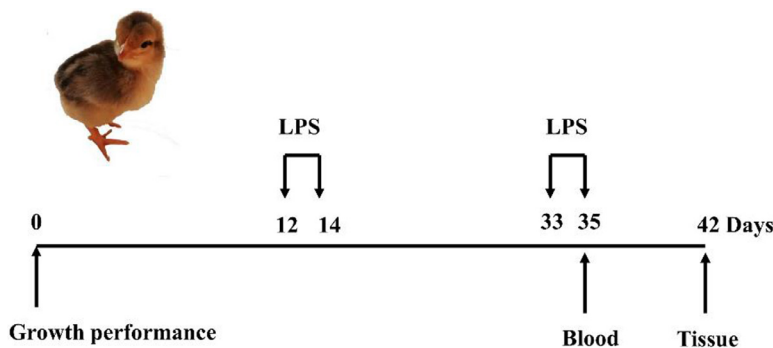
Figure 1. Details of the experimental schedule for model construction and sampling design. Black arrows above the timeline indicate the time points of lipopolysaccharide injection.

ACTH were determined by using ELISA kits according to the manufacturer's instructions.

Transcriptomic Analysis

A total of four samples per group were chosen at random and used in transcriptomics. The liver samples were stored at $-80°C$ for further investigation. The next generation sequencing experiments were performed by Allwegene Technology Co., Ltd. (Beijing, China). Briefly, total RNA was extracted using the TRIzol method (TIANGEN BIOTECH, Beijing) and quantified using Agilent 2100 Bioanalyzer (Agilent Technologies, CA) and NanoDrop spectrophotometer (IMPLEN, CA). Then sequencing libraries were generated using NEBNext Ultra RNA Library Prep Kit for Illumina (NEB) following manufacturer's recommendations and sequenced on an Illumina Hiseq 4000 platform. HTSeq v 0.5.4 p3 was used to count the reads numbers mapped to each gene. Gene expression levels were estimated by fragments per kilobase of transcript per million fragments mapped (**FPKM**). Genes with an adjusted P-value < 0.05 ($q < 0.05$) found by DESeq were identified as differentially expressed genes. Gene Ontology (**GO**) enrichment analysis of the differentially expressed genes (**DEGs**) was implemented by the GOseq R packages and Kyoto Encyclopedia of Genes and Genomes (**KEGG**) pathway enrichment analysis was performed using the KEGG Orthology-Based Annotation System (**KOBAS**).

Metabolite Extraction

Eight samples were employed from each group for the metabolomics experiments. The methods were performed as previously described (Cai et al., 2015). About 25 mg of sample was removed to a 1.5 mL EP tube, and 500 μL extract solution (methanol: acetonitrile: water = 2: 2: 1, with isotopically labeled internal standard mixture) was added into the tube. Then the samples were homogenized at 35 Hz for 4 min and sonicated for 5 min in ice-water bath. After that, the homogenization and sonication process were repeated for 3 times. The samples were then incubated for 1 h at $-40°C$ and centrifuged at 12,000 rpm for 15 min at $4°C$. The supernatant was transferred to a new fresh glass vial for analysis. The quality control (**QC**) sample was prepared by mixing an equal aliquot of the supernatants from all of the samples.

LC-MS/MS Analysis

An UHPLC system (Vanquish, Thermo Fisher Scientific, Waltham, MA) with a UPLC BEH Amide column (2.1 mm × 100 mm, 1.7 μm) coupled to Q Exactive HFX mass spectrometer (Orbitrap MS, Thermo, Waltham, MA) was employed to perform LC-MS/MS analyses. The mobile phase was composed of 25 mmol/L ammonium acetate and 25 mmol/L ammonia hydroxide in water (pH = 9.75) (A) and acetonitrile (B). The autosampler temperature was set at $4°C$, and the injection volume was 3 μL. The QE HFX mass spectrometer was applied for the purpose of acquiring MS/MS spectra on information-dependent acquisition (**IDA**) mode subject to the acquisition software (Xcalibur, Thermo, Waltham, MA). In this mode, the acquisition software continuously determines the full scan MS spectrum. The ESI source conditions were set as following: sheath gas flow rate as 30 Arb, Aux gas flow rate as 25 Arb, capillary temperature $350°C$, full MS resolution as 60,000, MS/MS resolution as 7,500, collision energy as 10/30/60 in NCE mode, spray Voltage as 3.6 kV (positive) or -3.2 kV (negative), respectively (Cai et al., 2015).

Metabolomic Data Analysis

ProteoWizard was used to transform the raw data to the mzXML format. Then an in-house program based on XCMS and developed using R was utilized for peak detection, extraction, alignment, and integration (Smith et al., 2006). Finally, an in-house MS2 database (BiotreeDB) was used in metabolite annotation. The cutoff for annotation was set at 0.3.

The resulted 3-dimensional data involving the peak number, sample name, and normalized peak area were fed to R package metaX (Wen et al., 2017) for principal component analysis (**PCA**) and orthogonal partial least squares discriminant analysis (**OPLS-DA**). A criterion that variable importance in the projection (**VIP > 1**) and $P < 0.05$ (student t-test) were set to identify

significantly changed metabolites. Moreover, KEGG (http://www.kegg.jp) and MetaboAnalyst (http://www.metaboanalyst.ca/) were applied to investigate the pathways of metabolites.

Quantitative Real-Time PCR

The total RNA was converted into cDNA using PrimeScriptRT Master Mix (Takara, Dalian, China) on a T100 thermal cycler (*Bio-Rad* Laboratories, Hercules, CA). RT-qPCR on selected genes using SYBRPremix Ex Taq II (Tli RNaseH Plus) (Takara, Dalian, China) was carried out on a Multiple Real-Time PCR System (AB, CA). The data were analyzed with $2^{-\Delta\Delta Ct}$ method and normalized to β-actin expression (Jiang et al., 2020). Information of primers were provided in Table S1.

Statistical Analysis

The data were analyzed by independent-samples *t*-test using SPSS software (version 17.0, SPSS Inc., Chicago, IL). Results are presented as mean ± standard error (**SE**). Differences between means at $P < 0.05$ or $P < 0.01$ were statistically significant. Genes from different samples were considered to be significantly changed in their abundance when they attained the criteria (*q*-value < 0.05). A criterion that VIP > 1 and $P < 0.05$ (student *t*-test) were set to identify significantly changed metabolites. The integrated network analysis of differential metabolites and DEGs were constructed using Metscape, a Cytoscape software (v3.7.1) plugin.

RESULTS
Validation of Immune Stress Model

The effect of immune stress on growth performance of broiler chicks was shown in Table 2. The LPS challenge significantly decreased DWG ($P < 0.01$) and DFI ($P < 0.01$) of broilers during 7-21 d, 22-35 d, and 36-42 d, when compared with the Controls. However, there was no significant difference between Model and Control in FCR of broilers ($P > 0.05$). As shown in Table 2, significantly higher relative weight of liver ($P < 0.05$) and spleen ($P < 0.01$) and significantly lower relative weight of bursa ($P < 0.01$) were found in the Model broilers, when compared with the Control. In addition, the broilers with immune stress had increased concentration of serum ACTH ($P < 0.01$) and CORT ($P < 0.05$) (Table 3).

Overview of the Transcriptome Sequencing

More than 6.4 Gb raw data were obtained from the transcriptome resulting in 42.9 to 53.3 million total reads for each sample. An average of 88.78% clean reads from Model samples and an average of 89.33% clean reads from Control samples were concordantly mapped

Table 2. Growth performance and relative weights of organs.

Item	Control	Model	P-Value
Growth performance			
DWG (g)			
7−21 d	22.93 ± 0.39	20.29 ± 0.25	0.000
22−35 d	31.49 ± 0.34	28.94 ± 0.38	0.001
36−42 d	53.84 ± 1.42	45.07 ± 0.90	0.000
DFI (g)			
7−21 d	46.00 ± 0.65	41.35 ± 0.47	0.000
22−35 d	83.14 ± 1.05	77.90 ± 0.80	0.003
36−42 d	121.80 ± 2.86	104.38 ± 2.44	0.001
FCR			
7−21 d	2.01 ± 0.03	2.04 ± 0.01	0.302
22−35 d	2.64 ± 0.02	2.69 ± 0.03	0.214
36−42 d	2.27 ± 0.04	2.32 ± 0.02	0.330
Relative weights of organs (g/kg)			
RW of liver	24.79 ± 1.60	29.86 ± 1.10	0.026
RW of spleen	1.51 ± 0.06	2.82 ± 0.22	0.000
RW of bursa	4.54 ± 0.20	3.76 ± 0.11	0.006

Values were expressed as means ± standard error (SE) (n = 6).
Abbreviations: DFI, daily feed intake; DWG, average daily weight gain; FCR, feed conversion ratio; RW, relative weights.

to the chicken genome sequence, respectively (Table S2). FPKM method was used to spot the differentially expressed genes. By comparing the FPKM values of all genes, the overall gene expression levels of each group could be evaluated. The FPKM boxplot, FPKM density distribution, and FPKM violin diagram (Figure S1) suggested that the expression level in Model group was higher than that of Control group. Figure S2 represents a PCA plot showing the quadruplicates from each group clustering together, and it is possible to observe a difference between the Model and Control groups. The genes with $q < 0.05$ were considered as DEGs. The significantly altered genes were shown in Table S3. A total of 129 DEGs were identified between Model and Control group, 60 DEGs were up-regulated while 69 DEGs were down-regulated (Figure 2A). DEGs identified in biological replicates clustered together, indicating good reproducibility of treatments (Figure 2B). To validate the accuracy of the RNA-seq data, expression levels of 9 DEGs (*ALB, NOX4, PLA2G4B, ACOX1, CETP, OVT, IL4I1, SAA, ExFABP*) were quantified by using qRT-PCR. RNA-seq results showed that the expression trend of the DEGs between the Model and Control group was consistent in qRT-PCR results, and this confirmed the reliability of the sequencing data (Figure 2C). GO project was utilized to analyze the potential biological function of DEGs. In this study, the 30 most enriched GO terms classified by molecular function, cellular component and biological processes terms were listed in Figure 2D. Pathway analysis was subsequently carried

Table 3. The concentrations of serum ACTH and CORT in broilers.

Items	Control	Model	P-Value
ACTH (ng/L)	38.34 ± 1.68	47.20 ± 2.03	0.007
CORT (ng/ml)	199.07 ± 9.85	243.33 ± 11.03	0.014

ACTH, adrenocorticotropic hormone; CORT, corticosterone. Values are means ± SE (n = 6).
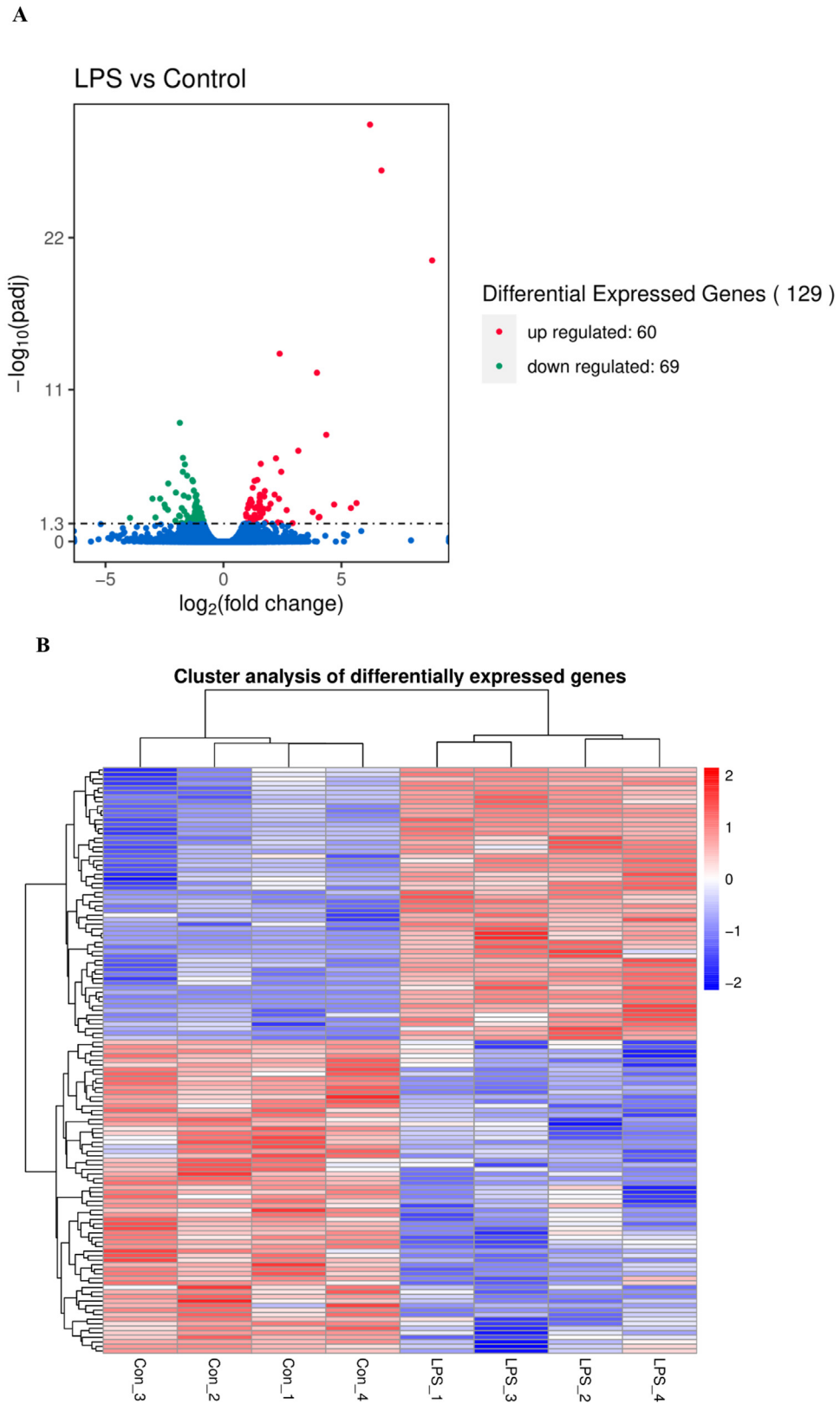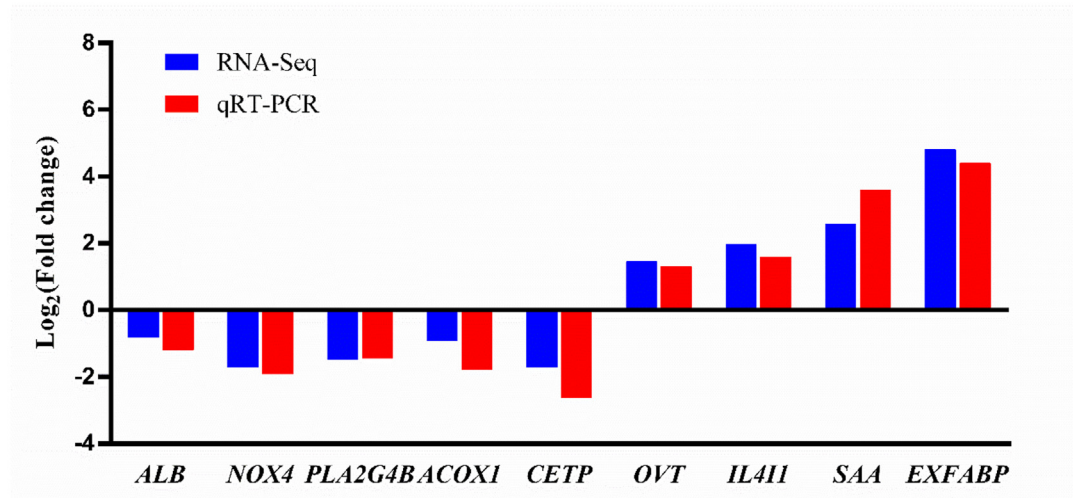
A

B

Figure 2. Analysis of differentially expressed genes. (A) Volcano plot of the DEGs; (B) Clustering map of the DEGs; (C) Comparison of gene expression data between RNA-Seq and qRT-PCR; (D) GO functional enrichment analysis of the DEGs; (E) KEGG pathway analysis of the DEGs.
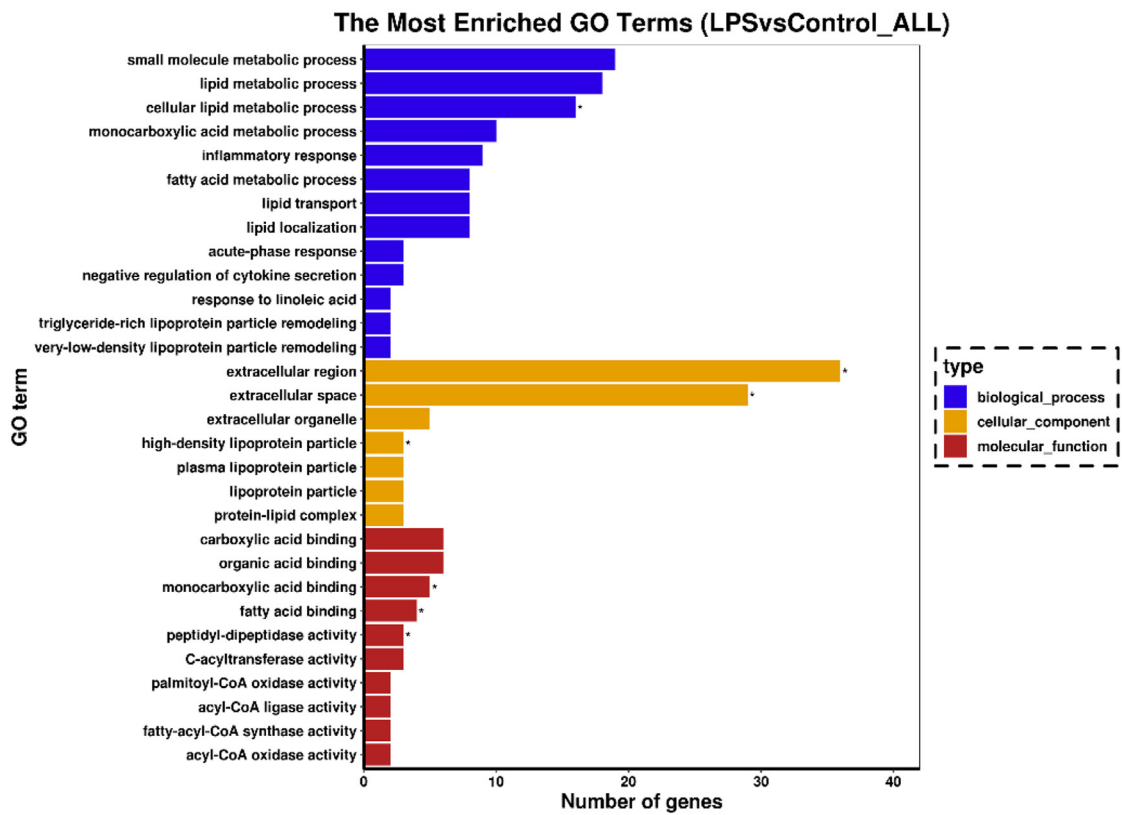
C
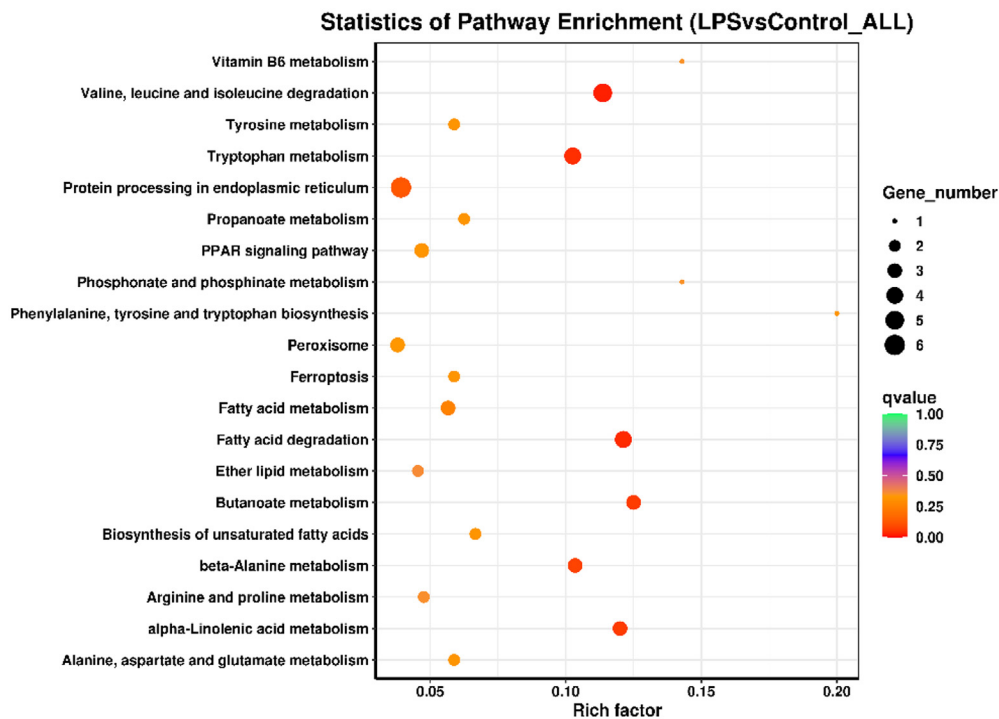

D

Figure 2 Continued.

E

Figure 2 Continued.

out on the basis of the KEGG. The top 20 pathways were represented in Figure 2E.

Metabolic Profiling Data

An OPLS-DA (Figure 3A) was performed on all analyzed metabolites to estimate the metabolic variance induced by LPS, which showed a clear discrimination between Model and Control subjects without any overlap ($R^2X = 24.8\%$, $R^2Y = 98.3\%$, $Q^2 = 69.4\%$), demonstrating a robust metabolic difference between the two groups. Validation using permutation test indicated that the model had not been overfitted (Figure 3B). A total of 109 differential metabolites were obtained base on VIP > 1 derives from the OPLS-DA model and $P < 0.05$ in t-test. Compared to the control group, 64 metabolites were up-regulated and 45 metabolites were down-regulated in Model group (Figure 3C). The significantly altered metabolites were shown in Table S4. A higher VIP value is correlated with a greater contribution of the corresponding metabolite to discriminating of Model and Control group and the top 20 metabolites discriminating the two groups are shown in Figure 3D. In order to identify possible pathways relevant to the broiler chicks with immune stress, all of the attributed metabolites were subjected to Metaboanalyst 3.0, a free online tool based on the high-quality KEGG metabolic pathways database (www.metaboanalyst.ca). The influenced

metabolic pathway was set as a pathway impact value > 0.25 or Raw_$P < 0.05$. As shown in Figure 3E, 10 metabolic pathways were significantly perturbed in Model group compared with Control group, embodying in amino acid metabolism (valine, leucine and isoleucine biosynthesis, biosynthesis of amino acids, histidine metabolism, glycine, serine, and threonine metabolism), lipid metabolism (glycerophospholipid metabolism), glycan metabolism (mucin type O-glycan biosynthesis, mannose type O-glycan biosynthesis) and metabolism of cofactors and vitamins (pantothenate and CoA biosynthesis). The other two biological modules included apoptosis and intestinal immune network for IgA production. The mucin type O-glycan biosynthesis and intestinal immune network for IgA production were significantly altered (Raw_$P < 0.05$) with high impact values (pathway impact > 0.25). Apoptosis as well as mannose type O-glycan biosynthesis was not significantly altered ($P > 0.05$) but with a high impact value. Other pathways were all markedly altered with low impact values.

Integrated Analysis of Transcriptomics and Metabolomics

The correlation analysis using the Pearson calculation to reveal the correlation between transcriptomics and metabolomics data. An overview of the DEGs and

A

B

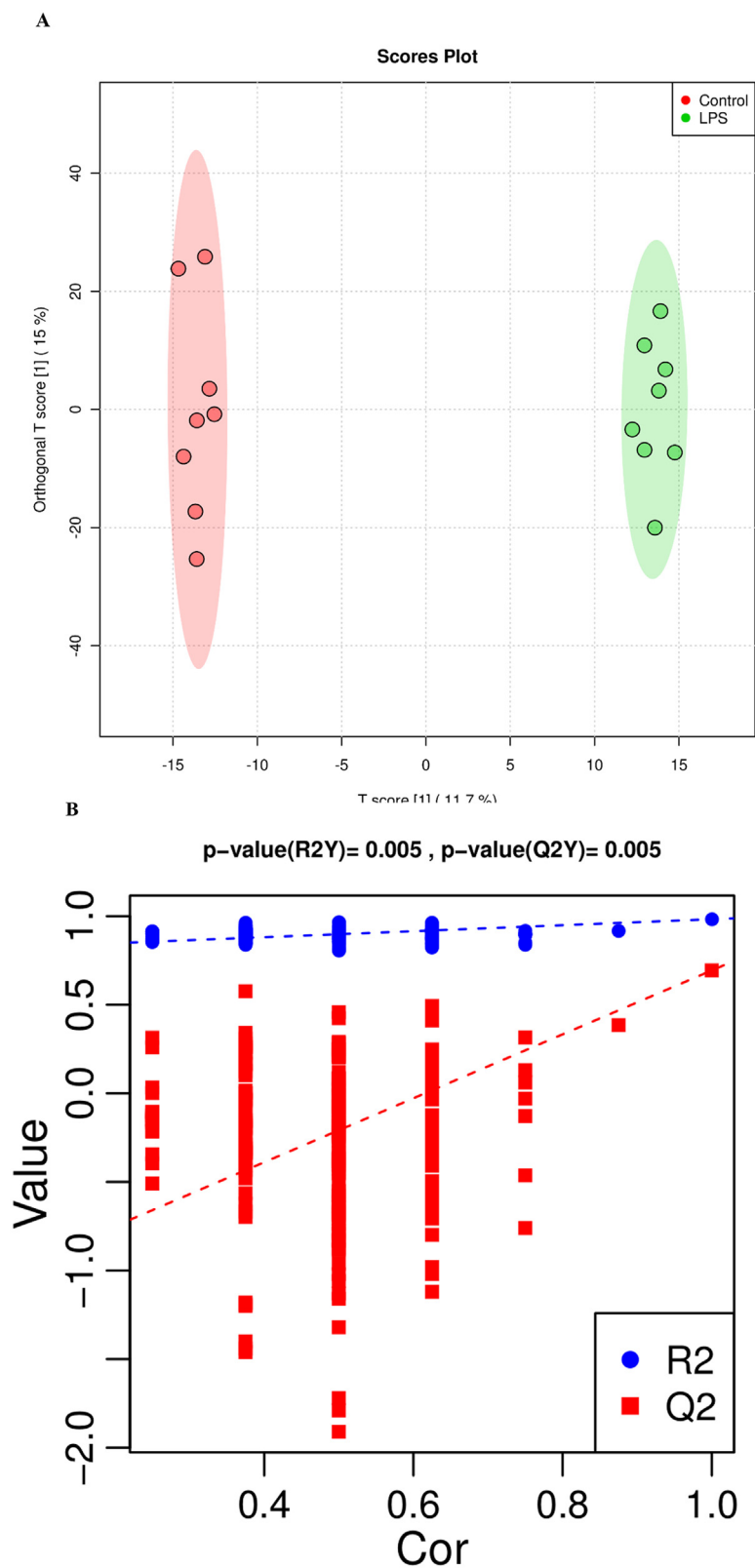**Figure 3.** Analysis of metabolic alterations of the Control and Model samples. (A) OPLS-DA score plots of metabolite profile; (B) Permutation test on the OPLS-DA model; (C) Hierarchical clustering of differential metabolites in the comparison Model vs. Control and (D) VIP plots from pairwise OPLS-DA analyses of groups: Model vs. Control; (E) Metabolome view from pathway analysis performed using MetaboAnalyst.

C

Cluster analysis of differential metabolites

D

Figure 3 Continued.

E

Statistics of Pathway Enrichment (LPSvsControl)
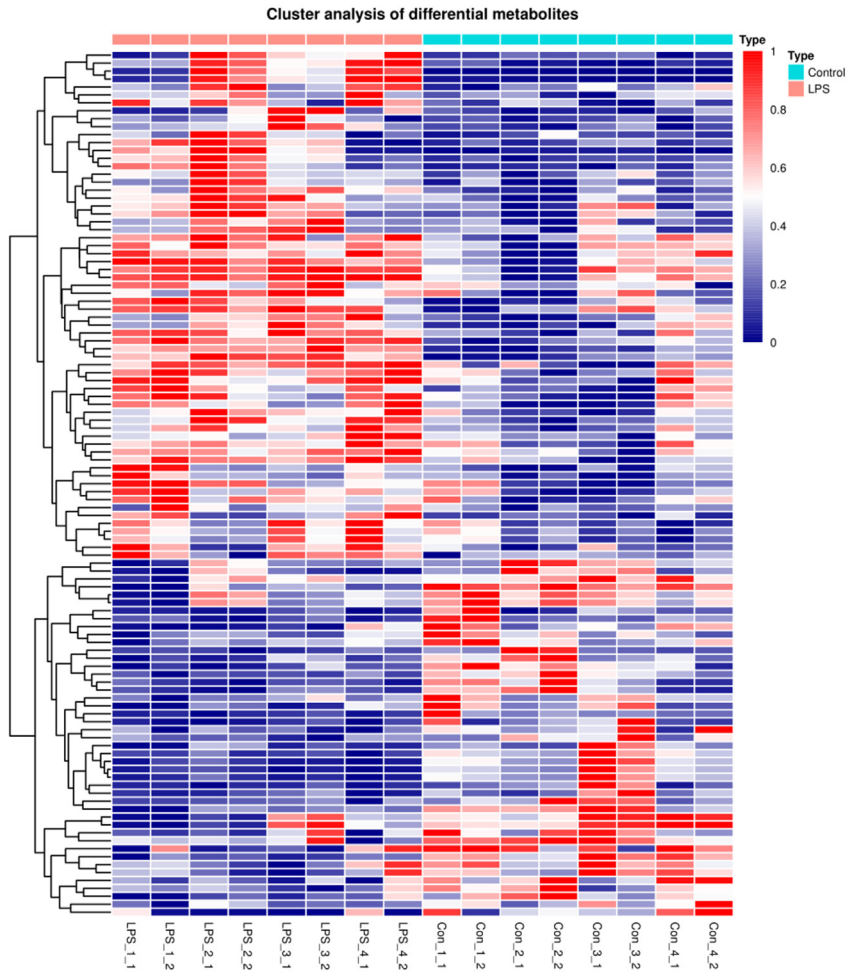
Figure 3 Continued.

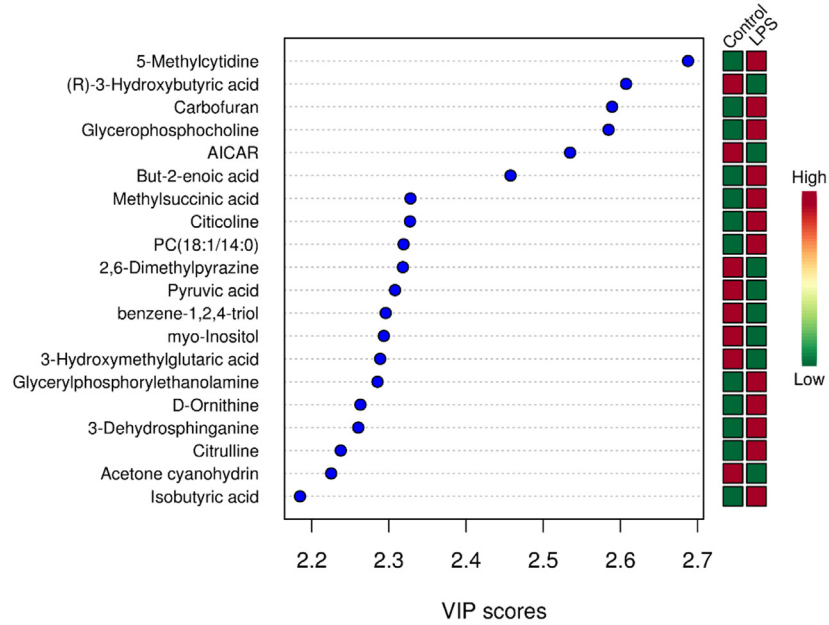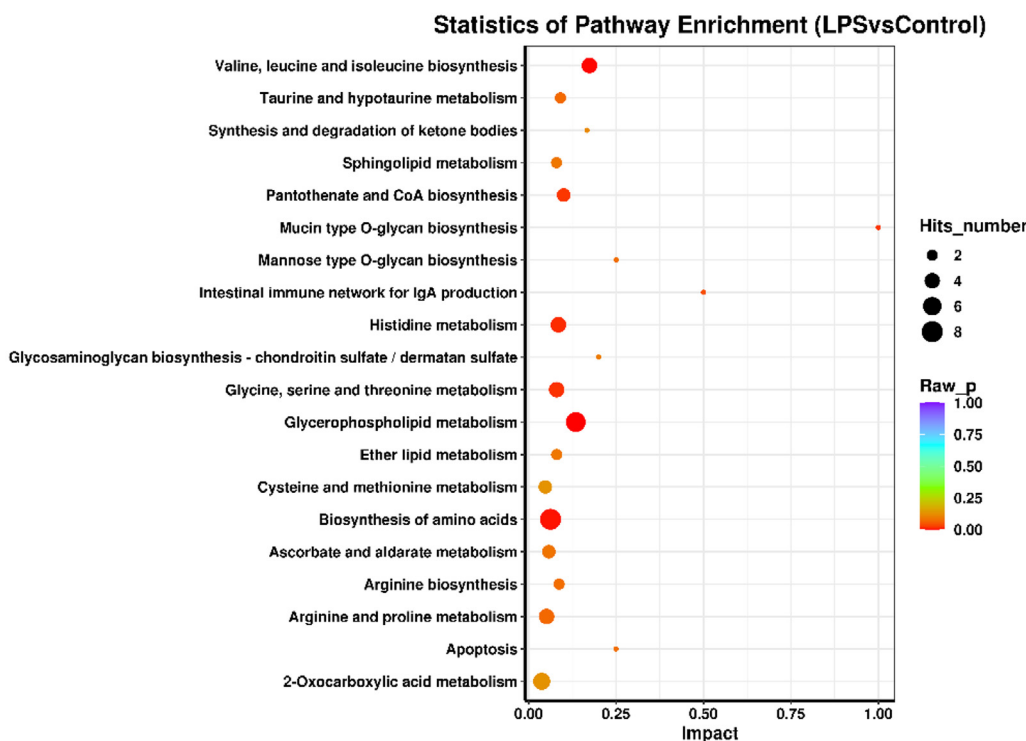differential metabolites found between Model and Control group was shown in Figure 4, which showed strong correlations between each transcript and metabolites. The altered genes and metabolites were combined to derive integrated signaling networks. One hundred nine altered metabolites and 129 changed genes were imported in Metsacpe to form a latent relationship network. Results indicated that there were two enriched metabolic pathways such as branched-chain amino acid metabolism (Figure 5A) and glycerophospholipid metabolism (Figure 5B). The integrated analysis of transcriptomics and metabolomics provided potential implications for understanding the systemic mechanism of LPS-induced immune stress.

DISCUSSION

The appetite and growth performance of the boiler chicken decline in response to an immune challenge (Liu et al., 2015). This could be explained by the fluctuation of serum ACTH and CORT levels related to the hypothalamus-pituitary-adrenal (**HPA**) axis (Zheng et al., 2016; Yang et al., 2021). Previous studies have demonstrated that LPS challenge induced increased inflammatory responses and stress-related hormone, resulting in decreased growth performance (Zheng et al., 2016; Li et al., 2018; Li et al., 2020). In

order to induce a chronic model of immune stress, a continuous interval injection of LPS was performed. The results showed that immune stress significantly decreased growth performance, induced higher relative weight of liver and spleen and lower relative weight of bursa, as well as increased concentration of serum ACTH and CORT. The data obtained here was in agreement with the previous studies (Morales-Lopez and Brufau, 2013; Shen et al., 2010; Liu et al., 2015; Ansari et al., 2017; Zhang et al., 2017a,b). Thus, in this experiment, a model of broiler chicks with immune stress and growth depression was successfully established. Simultaneously, we comprehensively applied biochemical analysis, transcriptomics, and metabolomics to compare the data between the model group and the control group. The results may help us clarify the pathogenesis of immune stress and search for potential therapeutic targets.

Amino acid metabolism

The alteration of nutrient metabolism is another cause of growth inhibition induced by immune stress. Under stress, the anabolism of body protein and fat is weakened while the catabolism of them is strengthened, in order to meet the needs for synthesis of immune effector molecules. Zheng et al. (2021) applied hepatic proteome and
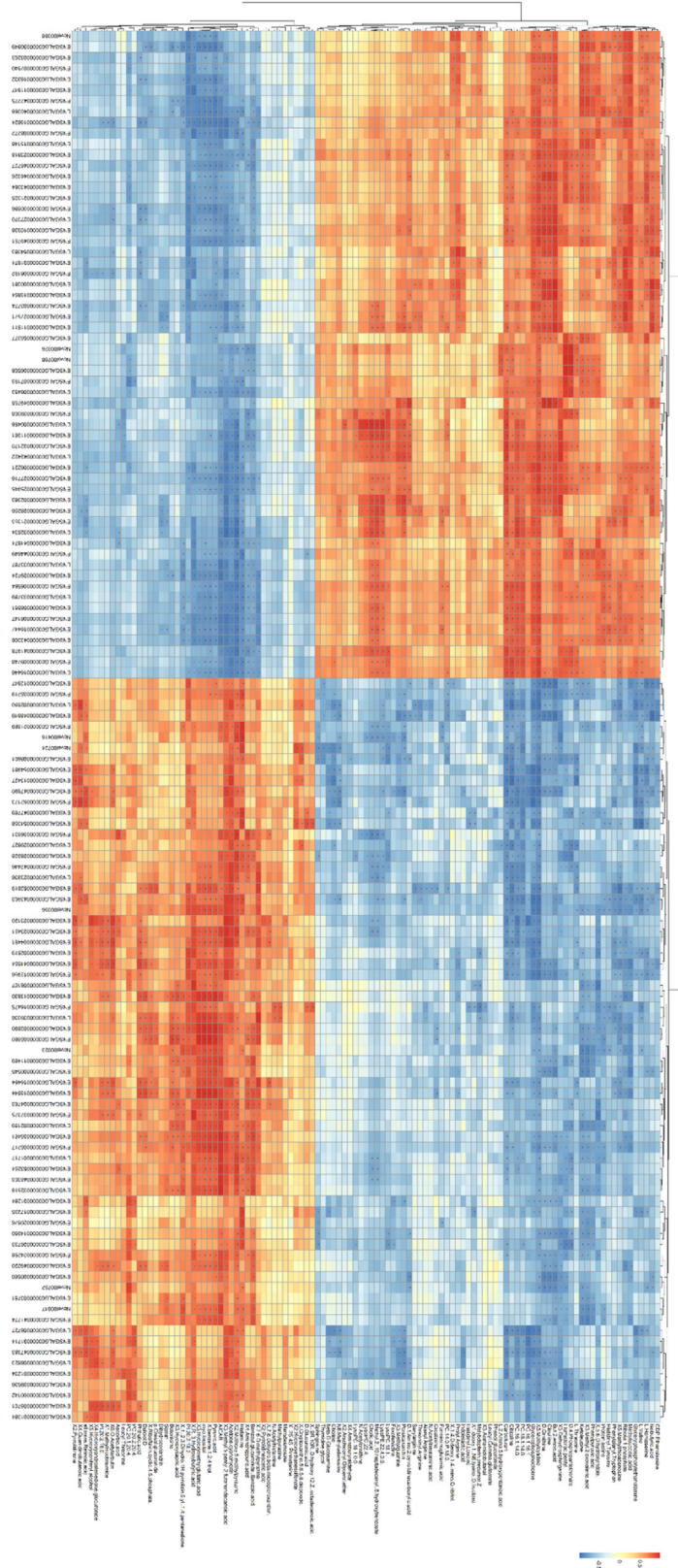
Figure 4. Heatmap of correlation between transcriptomics and metabolomics. The heatmap of genes in columns and metabolites in rows shows the relationship between genes and metabolites. Red and blue indicate positively correlated and negatively correlated related to transcriptomics and metabolomics. * indicates significant correlation ($P < 0.05$).

A

B

Figure 5. Metabolomic correlation networks of the differential metabolites (hexagons) and genes (rounds) represented in different dosage groups. Input metabolites were shown in red and input genes were shown in blue. The metabolic networks of valine, leucine and isoleucine biosynthesis (A); glycerophospholipid metabolism (B).

indicated that some proteins were significantly enriched in valine, leucine and isoleucine degradation pathway and organic acid catabolism processes. In this work, transcriptomic analysis showed that many DEGs were enriched in amino acid metabolism such as "valine, leucine, and isoleucine degradation," "tryptophan metabolism," "tyrosine metabolism," "phenylalanine, tyrosine, and tryptophan biosynthesis," "alanine, aspartate, and glutamate metabolism." Consistently, metabolomic analysis identified

differential metabolites in "amino acid metabolism," including L-Threonine, Pyruvic acid, L-Valine, Ketoleucine, Histamine, N-Acetylhistamine, Formiminoglutamic acid, Choline, L-Homoserine, N-Acetylornithine, Citrulline, AICAR, and Phenylpyruvic acid. L-threonine is the main limiting amino acid for poultry, which is of particular importance for the synthesis of acute phase proteins and immunoglobulins (Bi et al., 2018; Michael et al., 2018). If the L-threonine rise, the production of T and B

lymphocytes would be boosted to enhance immune responses (Yuan et al., 2017). Histamine is a mediator of inflammatory responses that are produced by mast cells, basophils, macrophages, and T lymphocytes. The present of histamine promoted dendritic cell migration, pro-inflammatory cytokine production, and Th2 cell activity (Coleman et al., 2020). In this study, L-threonine was significantly increased and histamine was significantly decreased in the liver from broilers with immune stress. Thus, it is probable that body protein was reduced to support promotion of immune responses and defense functions, declining feed utilization and growth performance.

Lipid Metabolism

Several studies reported that immune stress changed lipid metabolism in liver of broiler chickens. Han et al. (2020) showed that LPS challenge significantly increased MDA content, indicating that immune stress induced lipid peroxidation in the liver of broilers. A recent study demonstrated that differential proteins were significantly involved in fatty acid degradation, and lipid catabolic process, when compared the stress model and the Control broilers (Zheng et al., 2021). In this study, DEGs were enriched into lipid metabolism related terms including "lipid metabolic process," "fatty acid metabolic process," "lipid transport," "fatty acid binding," "fatty acid degradation," and "PPAR signaling pathway." PPAR signaling pathway is closely related to lipid metabolism and plays vital roles in regulation homeostasis of fatty acid uptake, oxidation, and lipid transport (Neve et al., 2000). In this study, *ACOX1, ACAA1*, and *EHHADH* were identified in the PPAR signaling pathway, all of them were downregulated. These results were similar with the previous studies and suggested that lipid metabolism in liver were significantly changed when broilers were subjected to immune stress (Zaytsoff et al., 2019; Li et al., 2021). Meanwhile, metabolomics analysis showed that changed metabolites were involved in glycerolphospholipid metabolism, such as LysoPC (18:1), Citicoline, Choline, PC (14:0/P-18:0), Glycerylphosphorylethanolamine, Glycerophosphocholine, CDP-Ethanolamine. Glycerophospholipids played a critical role in cell proliferation, apoptosis, and were recently reported to be a biomarker of liver injury and inflammatory response (Qiao et al., 2021). For example, LysoPCs, which generated from the hydrolysis of PCs, can induce the migration of lymphocytes and macrophages, increase the production of proinflammatory cytokines, induce oxidative stress, and promote apoptosis, which can aggregate inflammation and promote the development of diseases (Riederer et al., 2011; Liu et al., 2020). The mechanism by which LysoPC induces inflammatory factors is involved in the NF-κB, Notch, and PI3K/Akt signaling pathways (Liu et al., 2020). LysoPC also increases ROS generation

and inhibits NO, superoxide dismutase, and glutathione peroxidase production, which promotes caspase-3 activation and induces apoptosis (Park et al., 2010; Tsai et al., 2018). In the current study, immune stress significantly increased seven glycerophospholipid metabolites in the liver. This result suggested that elevation of glycerophospholipid would be a potential biomarker for the early detection of LPS-induced immune stress.

Inflammatory Response

Inflammatory response was generally known as hallmark of immune stress (Liu et al., 2015). Our previous study showed that the LPS challenge promoted the inflammatory response by increasing the content of serum IL-6, TNF-α, iNOS, and NO in broilers (Bi et al., 2022). In the present study, 8 DEGs (*SAA, BPIL, ANXA1, CCL19, CXCL13L2, EXFABP, IL1R2, IL22RA2*) of inflammatory response were upregulated and *FFAR4* was downregulated in liver of broiler chicken with stress. Except for the inflammatory response, immune stress also upregulated the DEGs of "acute-phase response," "response to stress," which were responsible for the defense function. Similarly, transcriptome analysis on bursa of chickens with stress also showed genes involved in "defense response," "immune response" (Zhang et al., 2018). At the same time, KEGG enrichment analysis of metabolomics showed significant changes in sphingolipid metabolism, arginine, and proline metabolism, which were associated with the inflammatory response. Sphingolipid metabolism is pivotal in the regulation of inflammatory signaling pathways (Norris and Blesso, 2017). The temporal switch of arginine as a substrate for the cytostatic iNOS/NO axis to the pro-growth arginase/ornithine/polyamine and proline axis is subject to regulation by inflammatory cytokines as well as interregulation by the arginine metabolites themselves (Satriano, 2004). In this study, 3-Dehydrosphinganine, Sphingosine in Sphingolipid metabolism were significantly upregulated, 4-Aminobutyraldehyde, Creatinine, 4-Guanidinobutanoic acid and Pyruvic acid in arginine and proline metabolism were significantly changed. The results suggested that decreased nutrition and metabolites were associated with activated inflammatory response and defense response. Indeed, there is evidence that several amino acids for muscle synthesis and growth was utilized for maintain inflammation in a bird model (Liu et al., 2015).

Oxidative Stress

Overproduction of proinflammatory cytokines can generate ROS, ultimately inflicting oxidative injury in multiple organ systems (Sasaki and Joh, 2007). Previous studies have observed that LPS challenge induced

oxidative stress and cause injury in brain, lung, spleen, thymus, and liver, resulting in dysfunction of multiple organs (Gorąca et al., 2013; Shah et al., 2017; Tanaka et al., 2017; Yang et al., 2019; Ding et al., 2021). In this study, the mRNA expression related to oxidoreductase activity (*ALDH3A2, AOX2, ACAA1, ACOX1, PDPR, EHHADH, NOX4, DMGDH*) in liver was downregulated by immune stress. The results of our data on gene expression are consistent with previous published studies, indicating that oxidative damage should also be considered in the pathogenesis of immune stress and growth inhibition (Han et al., 2020; Bi et al., 2022). A recent study using transcriptome identified several genes related to "antioxidant activity" in thymus of chicken response to stress (Tian et al., 2021).

BCAAs and mTOR Signaling Pathway

Using Metscape, compound reaction networks of the metabolites, genes were visualized to indicate the systemic mechanism of LPS-induced stress. Those metabolites and DEGs were mainly clustered in metabolic pathways of Valine, leucine, and isoleucine metabolism and Glycerophospholipid metabolism. In animals, BCAAs like leucine, isoleucine, and valine play important roles in energy balance, nutrition metabolism, gut health and immunity (Nie et al., 2018). The BCAAs act as substrates for protein synthesis or energy production, as well as perform a variety of metabolic and signaling functions, most notably through activating the mTOR signaling pathway (Holecek, 2018). In this study, four DEGs (*IL4I1, ACAA1, EHHADH,* and *ALDH3A2*) and three metabolites (valine, ketoisoleucine, and ketoleucine) participated in the compound-gene interactions of valine, leucine, and isoleucine metabolism. Interleukin 4 induced 1 (**IL4I1**) that also plays a role in the L-phenylalanine as well as L-tryptophan catabolic process. Previous study demonstrated that LPS challenge upregulated valine, leucine and isoleucine degradation pathway and IL4I1 was increased in the liver of broilers (Zheng et al., 2021), which is in accordance with the findings obtained here. Among the three BCAA, leucine earns the greatest reputation for its specific function in activation of the mTOR signaling pathway (Zhang et al., 2017a,b; Neinast et al., 2019). In this study, we found a decreased leucine level ($P > 0.05$) and an increased level of its downstream product ketoleucine ($P < 0.05$) in the liver of broilers with immune stress. The results were consistent with our previous study on mRNA expression of *mTOR, Akt,* and *PI3K* and strongly suggested that the inhibition of mTOR pathway is closely associated with the BCAA metabolism during immune stress (Bi et al., 2022). We speculated that lower leucine concentrations might contribute to mTOR inhibition in the liver.

CONCLUSIONS

In summary, the current study investigated the integrated profiling of hepatic transcriptomics and metabolomics in broiler chicks with immune stress. The results revealed number of DEGs and several metabolites that might account for amino acid metabolism, lipid metabolism, defense function, inflammatory response, and oxidation-reduction. We proposed that the pathogenesis of immune stress in broilers is associated with BCAA metabolism and through mTOR signaling pathway.

ACKNOWLEDGMENTS

DISCLOSURES

The authors declare no competing financial interests.

NOTE

The raw sequence data have been submitted to NCBI SRA (SAMN28772404-SAMN28772419), the raw metabolomics data have been deposited in the MetaboLights public repository under accession code MTBLS4996.

SUPPLEMENTARY MATERIALS

Supplementary material associated with this article can be found in the online version at doi:10.1016/j.psj.2022.102199.

REFERENCES

Ansari, A. R., N. Y. Li, Z. J. Sun, H. B. Huang, X. Zhao, L. Cui, Y. F. Hu, J. M. Zhong, N. A. Karrow, and H. Z. Liu. 2017. Lipopolysaccharide induces acute bursal atrophy in broiler chicks by activating TLR4-MAPK-NF-κB/AP-1 signaling. Oncotarget 8:108375–108391.

Bi, S., S. Ma, J. Wang, X. Chi, Y. Zhang, W. Xu, and S. Hu. 2019. Protective effect of Ginsenoside Rg1 on oxidative damage induced by hydrogen peroxide in chicken splenic lymphocytes. Oxid. Med. Cell. Longev. 2019:8465030.

Bi, S., Y. Qu, J. Shao, J. Zhang, W. Li, L. Zhang, J. Ni, and L. Cao. 2022. Ginsenoside Rg3 ameliorates stress of broiler chicks induced by Escherichia coli lipopolysaccharide. Front. Vet. Sci. 9:878018.

Bi, Y., X. M. Nan, S. S. Zheng, L. S. Jiang, and B. H. Xiong. 2018. Effects of dietary threonine and immune stress on growth performance, carcass trait, serum immune parameters, and intestinal muc2 and NF-kappab gene expression in Pekin ducks from hatch to 21 days. Poult. Sci. 97:177–187.

Cai, Y., K. Weng, Y. Guo, J. Peng, and Z. J. Zhu. 2015. An integrated targeted metabolomic platform for high-throughput metabolite profiling and automated data processing. Metabolomics 11:1575–1586.

Coleman, D. N., V. Lopreiato, A. Alharthi, and J. J. Loor. 2020. Amino acids and the regulation of oxidative stress and immune function in dairy cattle. J. Anim. Sci. 98:S175–S193.

Ding, D., D. Mou, L. Zhao, X. Jiang, L. Che, Z. Fang, S. Xu, Y. Lin, Y. Zhuo, J. Li, C. Huang, Y. Zou, L. Li, D. Wu, and B. Feng. 2021. Maternal organic selenium supplementation alleviates LPS induced inflammation, autophagy and ER stress in the thymus and spleen of offspring piglets by improving the expression of selenoproteins. Food Funct. 12:11214–11228.

Feng, B., S. Wu, F. Liu, Y. Gao, F. Dong, and L. Wei. 2013. Metabonomic analysis of liver tissue from BALB/c mice with D-galactosamine/lipopolysaccharide-induced acute hepatic failure. BMC Gastroenterol. 13:73.

Feed Database in China. 2013. Tables of feed composition and nutritive values in China. Feed Database in China, Beijing.

Gorąca, A., H. Huk-Kolega, P. Kleniewska, A. Piechota-Polańczyk, and B. Skibska. 2013. Effects of lipoic acid on spleen oxidative stress after LPS administration. Pharmacol. Rep. 65:179–186.

Han, H., J. Zhang, Y. Chen, M. Shen, E. Yan, C. Wei, C. Yu, L. Zhang, and T. Wang. 2020. Dietary taurine supplementation attenuates lipopolysaccharide-induced inflammatory responses and oxidative stress of broiler chickens at an early age. J. Anim. Sci. 98:skaa311.

Hasin, Y., M. Seldin, and A. Lusis. 2017. Multi-omics approaches to disease. Genome Biol. 18:83.

Hennigar, S. R., J. P. McClung, and S. M. Pasiakos. 2017. Nutritional interventions and the IL-6 response to exercise. FASEB J. 31:3719–3728.

Holecek, M. 2018. Branched-chain amino acids in health and disease: metabolism, alterations in blood plasma, and as supplements. Nutr. Metab. 15:33.

Jiang, J., S. Liu, T. Jamal, T. Ding, L. Qi, Z. Lv, D. Yu, and F. Shi. 2020. Effects of dietary sweeteners supplementation on growth performance, serum biochemicals, and jejunal physiological functions of broiler chickens. Poult. Sci. 99:3948–3958.

Li, J., Y. Cheng, Y. Chen, H. Qu, Y. Zhao, C. Wen, and Y. Zhou. 2019. Dietary chitooligosaccharide inclusion as an alternative to antibiotics improves intestinal morphology, barrier function, antioxidant capacity, and immunity of broilers at early age. Animals 9:493.

Li, R. F., S. P. Liu, Z. H. Yuan, J. E. Yi, Y. N. Tian, J. Wu, and L. X. Wen. 2020. Effects of induced stress from the live LaSota Newcastle disease vaccination on the growth performance and immune function in broiler chickens. Poult. Sci. 99:1896–1905.

Li, R., Z. Song, J. Zhao, D. Huo, Z. Fan, D. Hou, and X. He. 2018. Dietary L-theanine alleviated lipopolysaccharide-induced immunological stress in yellow-feathered broilers. Anim. Nutr. 4:265–272.

Li, X., S. Liu, J. Wang, J. Yi, Z. Yuan, J. Wu, L. Wen, and R. Li. 2021. Effects of ND vaccination combined LPS on growth performance, antioxidant performance and lipid metabolism of broiler. Res. Vet. Sci. 135:317–323.

Liu, L., J. Shen, C. Zhao, X. Wang, J. Yao, Y. Gong, and X. Yang. 2015. Dietary Astragalus polysaccharide alleviated immunological stress in broilers exposed to lipopolysaccharide. Int. J. Biol. Macromol. 72:624–632.

Liu, P. P., W. Zhu, C. Chen, B. Yan, L. Zhu, X. Chen, and C. Peng. 2020. The mechanisms of lysophosphatidylcholine in the development of diseases. Life Sci. 247:117443.

Liu, S. Q., L. Y. Wang, G. H. Liu, D. Z. Tang, X. X. Fan, J. P. Zhao, H. C. Jiao, X. J. Wang, S. H. Sun, and H. Lin. 2018. Leucine alters immunoglobulin a secretion and inflammatory cytokine expression induced by lipopolysaccharide via the nuclear factor-κB pathway in intestine of chicken embryos. Animal 12:1903–1911.

Michael, O. W., K. H. John, G. V. K. Andrew, and A. C. Daniel. 2018. Impact of dietary fiber and immune system stimulation on

threonine requirement for protein deposition in growing pigs. J. Anim. Sci. 96:5222–5232.

Morales-Lopez, R., and J. Brufau. 2013. Immune-modulatory effects of dietary Saccharomyces cerevisiae cell wall in broiler chickens inoculated with Escherichia coli lipopolysaccharide. Br. Poult. Sci. 54:247–251.

Neinast, M., D. Murashige, and Z. Arany. 2019. Branched chain amino acids. Annu. Rev. Physiol. 81:139–164.

Neve, B. P., J. C. Fruchart, and B. Staels. 2000. Role of the peroxisome proliferator-activated receptors (PPAR) in atherosclerosis. Biochem. Pharmacol. 60:1245–1250.

Nie, C., T. He, W. Zhang, G. Zhang, and X. Ma. 2018. Branched chain amino acids: beyond nutrition metabolism. Int. J. Mol. Sci. 19:954.

Norris, G. H., and C. N. Blesso. 2017. Dietary and endogenous sphingolipid metabolism in chronic inflammation. Nutrients 9:1180.

Park, S., J. A. Kim, S. Choi, and S. H. Suh. 2010. Superoxide is a potential culprit of caspase-3 dependent endothelial cell death induced by lysophosphatidylcholine. J. Physiol. Pharmacol. 61:375–381.

Patel, H. J., and B. M. Patel. 2017. TNF-α and cancer cachexia: Molecular insights and clinical implications. Life Sci. 170:56–63.

Qiao, N., Y. Y. Yang, J. Z. Liao, H. Zhang, F. Yang, F. Y. Ma, Q. Y. Han, W. L. Yu, Y. Li, L. M. Hu, J. Q. Pan, R. Hussain, and Z. X. Tang. 2021. Metabolomics and transcriptomics indicated the molecular targets of copper to the pig kidney. Ecotoxicol. Environ. Saf. 218:112284.

Riederer, M., M. Lechleitner, A. Hrzenjak, H. Koefeler, G. Desoye, A. Heinemann, and S. Frank. 2011. Endothelial lipase (EL) and EL-generated lysophosphatidylcholines promote IL-8 expression in endothelial cells. Atherosclerosis 214:338–344.

Sasaki, M., and T. Joh. 2007. Oxidative stress and ischemia-reperfusion injury in gastrointestinal tract and antioxidant, protective agents. J. Clin. Biochem. Nutr. 40:1–12.

Satriano, J. 2004. Arginine pathways and the inflammatory response: interregulation of nitric oxide and polyamines: review article. Amino Acids 26:321–329.

Shah, S. A., M. Khan, M. Jo, M. G. Jo, F. U. Amin, and M. O. Kim. 2017. Melatonin stimulates the SIRT1/Nrf2 signaling pathway counteracting lipopolysaccharide (LPS)-induced oxidative stress to rescue postnatal rat brain. CNS Neurosci. Ther. 23:33–44.

Shen, Y. B., X. S. Piao, S. W. Kim, L. Wang, and P. Liu. 2010. The effects of berberine on the magnitude of the acute inflammatory response induced by Escherichia coli lipopolysaccharide in broiler chickens. Poult. Sci. 89:13–19.

Smith, C. A., E. J. Want, G. O'Maille, R. Abagyan, and G. Siuzdak. 2006. XCMS: processing mass spectrometry data for metabolite profiling using nonlinear peak alignment, matching, and identification. Anal. Chem. 78:779–787.

Tanaka, K., T. Sugizaki, Y. Kanda, F. Tamura, T. Niino, and M. Kawahara. 2017. Preventive effects of carnosine on lipopolysaccharide-induced lung injury. Sci. Rep. 7:42813.

Tian, H., Y. Guo, M. Ding, A. Su, W. Li, Y. Tian, K. Li, G. Sun, R. Jiang, R. Han, F. Yan, and X. Kang. 2021. Identification of genes related to stress affecting thymus immune function in a chicken stress model using transcriptome analysis. Res. Vet. Sci. 138:90–99.

Tsai, T., I. Leong, K. Cheng, L. Shiao, T. Su, K. Wong, P. Chan, and Y. Leung. 2018. Lysophosphatidylcholine-induced cytotoxicity and protection by heparin in mouse brain bEND.3 endothelial cells. Fundam. Clin. Pharmacol. 33:52–62.

Wen, B., Z. Mei, C. Zeng, and S. Liu. 2017. metaX: a flexible and comprehensive software for processing metabolomics data. BMC Bioinformatics 18:183.

Xing, Y. Y., Y. K. Zheng, S. Yang, L. H. Zhang, S. W. Guo, L. L. Shi, Y. Q. Xu, X. Jin, S. M. Yan, and B. L. Shi. 2021. Artemisia ordosica polysaccharide alleviated lipopolysaccharide-induced oxidative stress of broilers via Nrf2/Keap1 and TLR4/NF-κB pathway. Ecotoxicol. Environ. Saf. 223:112566.

Yang, L., G. Liu, X. Liang, M. Wang, X. Zhu, Y. Luo, Y. Shang, J. Yang, P. Zhou, and X. Gu. 2019. Effects of berberine on the growth performance, antioxidative capacity and immune response to lipopolysaccharide challenge in broilers. Anim. Sci. J. 90:1229–1238.

Yang, S., J. Zhang, Y. Jiang, Y. Q. Xu, X. Jin, S. M. Yan, and B. L. Shi. 2021. Effects of Artemisia argyi flavonoids on growth performance and immune function in broilers challenged with lipopolysaccharide. Anim. Biosci. 34:1169–1180.

Yuan, A., L. Gong, L. Luo, J. Dang, X. Gong, M. Zhao, Y. Li, Y. Li, and C. Peng. 2017. Revealing anti-inflammation mechanism of water-extract and oil of forsythiae fructus on carrageenan-Induced edema rats by serum metabolomics. Biomed. Pharmacother. 95:929–937.

Zaytsoff, S., C. Brown, T. Montina, G. Metz, D. W. Abbott, R. Uwiera, and G. D. Inglis. 2019. Corticosterone-mediated physiological stress modulates hepatic lipid metabolism, metabolite profiles, and systemic responses in chickens. Sci. Rep. 9:19225.

Zhang, P. F., B. L. Shi, J. L. Su, Y. X. Yue, Z. X. Cao, W. B. Chu, K. Li, and S. M. Yan. 2017a. Relieving effect of Artemisia argyi aqueous extract on immune stress in broilers. J. Anim. Physiol. Anim. Nutr. 101:251–258.

Zhang, S., X. Zeng, M. Ren, X. Mao, and S. Qiao. 2017b. Novel metabolic and physiological functions of branched chain amino acids: a review. J. Anim. Sci. Biotechnol. 8:10.

Zhao, J., C. Xie, K. L. Wang, S. Takahashi, K. W. Krausz, D. S. Lu, Q. Wang, Y. H. Luo, G. X. Gong, X. Y. Mu, Q. Wang, S. W. Su, and F. J. Gonzalez. 2020. Comprehensive analysis of transcriptomics and metabolomics to understand triptolide-induced liver injury in mice. Toxicol. Lett. 333:290–302.

Zhang, Y., Y. Zhou, G. Sun, K. Li, Z. Li, A. Su, X. Liu, G. Li, R. Jiang, R. Han, Y. Tian, X. Kang, and F. Yan. 2018. Transcriptome profile in bursa of Fabricius reveals potential mode for stress-influenced immune function in chicken stress model. BMC Genomics 19:918.

Zheng, A., A. Zhang, Z. Chen, S. A. Pirzado, W. Chang, H. Cai, W. L. Bryden, and G. Liu. 2021. Molecular mechanisms of growth depression in broiler chickens (Gallus Gallus domesticus) mediated by immune stress: a hepatic proteome study. J. Anim. Sci. Biotechnol. 12:90.

Zheng, X. C., Q. J. Wu, Z. H. Song, H. Zhang, J. F. Zhang, L. L. Zhang, T. Y. Zhang, C. Wang, and T. Wang. 2016. Effects of Oridonin on growth performance and oxidative stress in broilers challenged with lipopolysaccharide. Poult. Sci. 95:2281–2289.